

DTIC FILE COPY

ATI-9163

Reg# R2543

UNCLASSIFIED

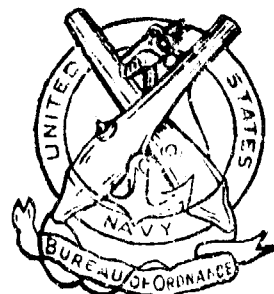
TECHNICAL LIBRARY FILE COPY NWL

NPG 3-44

AD-A955 280

U. S. NAVAL PROVING GROUND

Dahlgren, Virginia.



ORDNANCE LIBRARY
NPG, DAHLGREN, VA.

REPORT NO. 3-44

PENETRATION MECHANISMS

SUPPLEMENTARY REPORT ON THE PENETRATION
OF HOMOGENEOUS PLATE BY UNCAPPED PROJEC-
TILES AT 0° OBliquITY.

Approved for Public Release;
Distribution Unlimited.

24 February 1944.

DTIC
ELECTE
SEP 21 1987
S D

INDEXED	✓
DESCRIPTIVE	✓

UNCLASSIFIED

TECHNICAL LIBRARY FILE COPY NWL

87

9 10 109

Encl. (40)

DISCLAIMER NOTICE

**THIS DOCUMENT IS BEST QUALITY
PRACTICABLE. THE COPY FURNISHED
TO DTIC CONTAINED A SIGNIFICANT
NUMBER OF PAGES WHICH DO NOT
REPRODUCE LEGIBLY.**

C O P Y

SL3-1(3)(BEO 61896)

U. S. NAVAL PROVING GROUND,
DAHLGREN, VA.

UNCLASSIFIED

11 Mar 1944

From: The Commanding Officer.
To: The Chief of the Bureau of Ordnance.
Subject: NPG Report No. 3-44, Supplementary
Report on the Penetration of Homo-
geneous Plate by Uncapped Projectiles
at 0° Obliquity, Forwarding of.
References: (a) Buord ltr. NP9/A9 (Re3) dated
9 January, 1943.
(b) NPG Report No. 1-43.
Enclosure: (A) Twenty-five (25) Copies of
(S.C.) Subject Report.

1. By Enclosure (A), twenty-five (25) copies of Naval Proving Ground Report No. 3-44 are submitted under NPG Research Project APL-2 authorized in reference (a).

2. The subject report is a continuation of reference (b) and covers several special phenomena occurring in penetrations of homogeneous plate by uncapped projectiles at 0° obliquity. Analyses are given of the following:

- (1) Effect of velocity on impact dimensions.
- (2) Energy expended in projectile deformation.
- (3) Energy consumed in overcoming friction.
- (4) The hardness distribution surrounding partial and complete impacts.

UNCLASSIFIED

UNCLASSIFIED

U. S. NAVAL PROVING GROUND
Dahlgren, Virginia.

ORDNANCE LIBRARY
NPG, DAHLGREN, VA.

REPORT NO. 3-44

24 February 1944.

PENETRATION MECHANISMS

II. SUPPLEMENTARY REPORT ON THE PENETRATION
OF HOMOGENEOUS PLATE BY UNCAPPED PROJEC-
TILES AT 0° OBLIQUITY.

Accession For	
NTIS CRA&I	<input checked="checked" type="checkbox"/>
DTIC TAB	<input type="checkbox"/>
Unannounced	<input type="checkbox"/>
Justification	
By	
Distribution/	
Availability Codes	
Dist	Avail and/or Special
A-1	23



APPROVED:

David I. Hedrick
DAVID I. HEDRICK
CAPTAIN, USN
COMMANDING OFFICER

Page 1

UNANNOUNCED

UNCLASSIFIED

UNCLASSIFIED

P R E F A C E

AUTHORIZATION

This study is part of the program authorized in Bureau of Ordnance letter NP9/A9(Re3) dated 9 January, 1943, as Naval Proving Ground Research Project APL -2.

OBJECT

To extend the scope of Naval Proving Ground Report 1-43 on the mechanisms of armor penetration.

Page 11

UNCLASSIFIED

UNCLASSIFIED

SUMMARY

The penetration of homogeneous plate by uncapped projectiles at 0° obliquity was discussed in Naval Proving Ground Report No. 1-43. The present report supplements Report No. 1-43 with comments on four secondary features of penetrations of the same classification. They are:

1. The effect of velocity on impact dimensions, - an analysis of the energy absorption by the armor material as shown by the enlargement of the hole produced by completely penetrating projectiles of various velocities.
2. A measurement of the energy expended in deforming projectiles obtained by observation of the rise in temperature of the projectile.
3. An analysis of the energy consumed in overcoming friction between the projectile and plate by observation of the retardation in rotation as well as velocity.
4. A survey of the hardness distribution in sliced sections of armor surrounding partial and complete penetrations.

UNCLASSIFIED

UNCLASSIFIED

<u>CONTENTS</u>	<u>Page</u>
I. INTRODUCTION	1
II. EFFECT OF VELOCITY ON IMPACT DIMENSIONS	1
III. ENERGY EXPENDED IN PROJECTILE DEFORMATION ...	6
IV. FRICTION IN PROJECTILE IMPACT	7
V HARDNESS DISTRIBUTION AROUND IMPACTS	16

Page iv

UNCLASSIFIED

UNCLASSIFIED

LIST OF FIGURES

	<u>Opposite Page</u>
Fig. 1 - NPG Photo No. 1031 (APL).	3
Fig. 2 - NPG Photo No. 1054 (APL).	4
Fig. 3 - NPG Photo No. 1032 (APL).	4
Fig. 4 - NPG Photo No. 908 (APL).	7
Fig. 5 - NPG Photo No. 1004 (APL).	16
Fig. 6 - NPG Photo No. 1005 (APL).	16
Fig. 7 - NPG Photo No. 1006 (APL).	16
Fig. 8 - NPG Photo No. 1007 (APL).	16
Fig. 9 - NPG Photo No. 686 (APL).	16
Fig. 10 - NPG Photo No. 687 (APL).	16
Fig. 11 - NPG Photo No. 861 (APL).	16
Fig. 12 - NPG Photo No. 862 (APL).	16
Fig. 13 - NPG Photo No. 863 (APL).	16
Fig. 14 - NPG Photo No. 864 (APL).	16
Fig. 15 - NPG Photo No. 919 (APL).	16
Fig. 16 - NPG Photo No. 920 (APL).	16
Fig. 17 - NPG Photo No. 893 (APL).	16
Fig. 18 - NPG Photo No. 891 (APL).	16
Fig. 19 - NPG Photo No. 890 (APL).	16
Fig. 20 - NPG Photo No. 892 (APL).	16
Fig. 21 - NPG Photo No. 688 (APL).	16

UNCLASSIFIED

UNCLASSIFIED

I INTRODUCTION.

In reference (1) H. A. Bethe introduced a remarkably fruitful concept into the study of penetration mechanisms, namely, that provided the projectile is pointed the energy expended in making a hole in a plate is independent of the precise details of the process, and depends only upon the thickness of the plate and the size of the hole. In reference (2) it was shown that by a proper consideration of end-effects - mainly the formation of petals on the back of a homogeneous plate - the theory of reference (1) could be brought into reasonably good agreement with observation. It was also pointed out that blunt projectiles may be expected to penetrate a homogeneous plate by a punching mechanism, which is distinct in nature from the piercing-type of penetration required for the expanding-hole mechanisms of reference (1).

The method of Bethe has its limitations, and leaves out of consideration several important details, namely, the effect of striking velocity on the size of the hole in the plate and on the consequent energy absorption, the energy used in deformation of the projectile, and the effect of friction upon the energy of penetration. The present report discusses the available Proving Ground data bearing upon these points, and in addition presents data on etchings and hardness patterns made on sections through complete and incomplete penetrations of a heavy homogeneous plate. These etchings and hardness patterns were mentioned in reference (2) (p. 8), but were not ready for publication at the time that report was prepared.

II EFFECT OF VELOCITY ON IMPACT DIMENSIONS.

Disregarding frictional effects, the expanding hole theory and its modifications predict essentially the same size hole and the same energy absorption in the complete penetration of a plate, regardless of the velocity of penetration - i.e., the same result would be obtained if a projectile is pushed statically through a plate as when it is fired through.

A consideration of the details of the penetration process throws doubt on the correctness of this conclusion. In a dynamic penetration, as the point of the

UNCLASSIFIED

UNCLASSIFIED

projectile advances through the plate it must not only overcome the cohesion of the steel, but must set it in motion with a sufficient velocity so that it will move out of the way of the projectile. The point of the projectile must supply the necessary accelerating force, and so will experience a greater pressure than that required to overcome the static resistance. The dynamic term in the pressure will be of the order of magnitude of $(1/2) \rho v^2$, where ρ is the density of the armor plate, and v is the speed of the projectile. If

$$\begin{aligned} v &= 1500 \text{ ft./sec.}, \\ \rho &= 0.284 \text{ lb./in.}^3, \\ (1/2) \rho v^2 &= 1.2 \times 10^5 \text{ lb./in.}^2 \end{aligned}$$

The static yield-stress of heavy Class B plate of the usual hardness is around 10^5 lb./in.^2 and the static term in the pressure will be of this order of magnitude. It is thus seen that even at moderate velocities the dynamic term in the expression for the pressure near the point of a projectile may easily be equal to or larger than the pressure required for a static penetration.

Farther back along the ogive the pressure will be less, and in fact may fall below that which would exist in a static penetration. The situation is analogous to that which exists in the motion of a streamlined body through a resisting medium, and has been discussed by Zener and Peterson in reference (c). In a qualitative way one can see how the pressure must fall along the surface of the projectile nose from point to bourrelet.

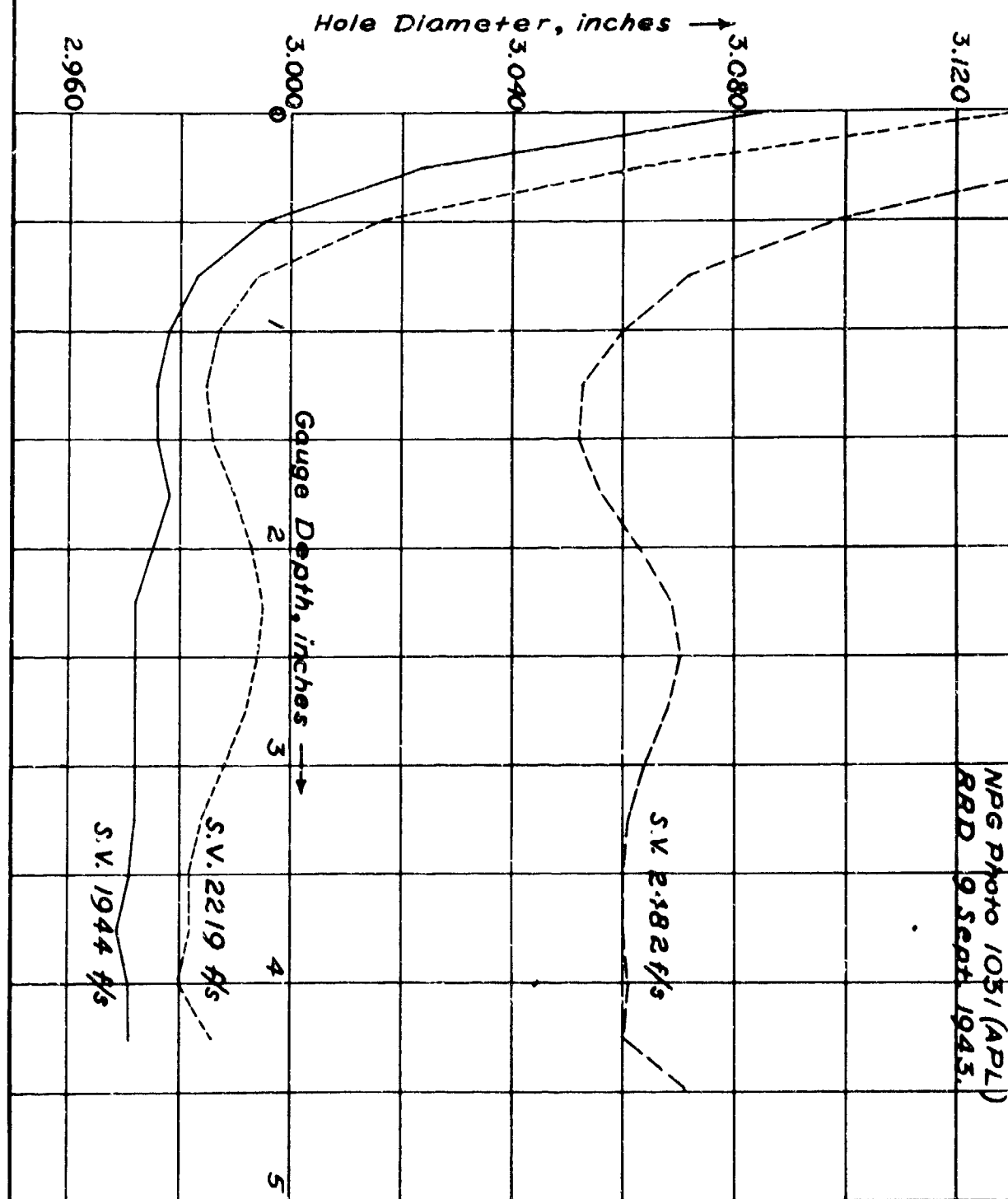
The material set in motion by the point of the projectile will tend, because of its inertia, to continue to expand, and less pressure by the ogive will be necessary to continue the expansion than in a static penetration.

An observation supporting this theory is that when an uncapped projectile is recovered after a complete penetration, the nose near the point is found to be wiped smooth and worked, while the last third of the nose near the bourrelet still has the tool marks and even some paint on it. This observation has been made on all projectiles emerging from the plate with a low velocity, or which tumbled after penetration (as in oblique impacts) so as

UNCLASSIFIED

DIAMETER OF IMPACT HOLES **3" AP M79 Projectiles vs. 4" Class B Plate at 0°**

The gauge depth is measured from the plane of the original face of the plate. All penetrations complete.



not to be scoured smooth in the sand of the butt, and has also been made on many projectiles rejected by the plate, although they had penetrated far enough to embed the bourrelet.

It seems possible that at high enough velocities and for at least part of the depth of the penetration-hole the inertial effect may cause the hole to continue to expand after passage of the bourrelet of the projectile. If this is the case, one would expect to find that

- (1) The hole in the plate will taper, being largest at the entrance and smallest at the exit end.
- (2) If several rounds are fired through a plate at different striking velocities, the holes will be largest for those rounds having the highest velocities.
- (3) The energy absorbed by the plate should increase with increased striking velocity and consequent greater hole size, according to the law for the limit energy, which is of the form

$$E_L = Ad^2 (e - kd) \dots \dots \dots (1)$$

(see reference (2), Sec. II). The value of the hole-diameter d to be used in this equation will be the mean value averaged through the thickness e of the plate. The appropriate numerical values of the constants A and k in Eq. (1) must be determined experimentally for the plate-hardness and the projectiles used; typical data, given in Fig. 1 of reference (2), are

$$A = 2.49 \times 10^4 \text{ ft. lbs./in.}^3, k = 0.132 \dots \dots (2)$$

for the 3" AP M-79 projectile vs. homogeneous plate of tensile strength from 110,000 to 130,000 p.s.i.

It is quite convenient to measure impact holes made by 3" projectiles by use of a star gauge used for gauging 3" guns. Fig. 1 of this report shows the results obtained on three holes made by 3" AP M-79 projectiles in a 4" Class B plate of hardness $R_C 19$, the striking velocities being respectively 1944, 2219 and 2482 ft./sec.

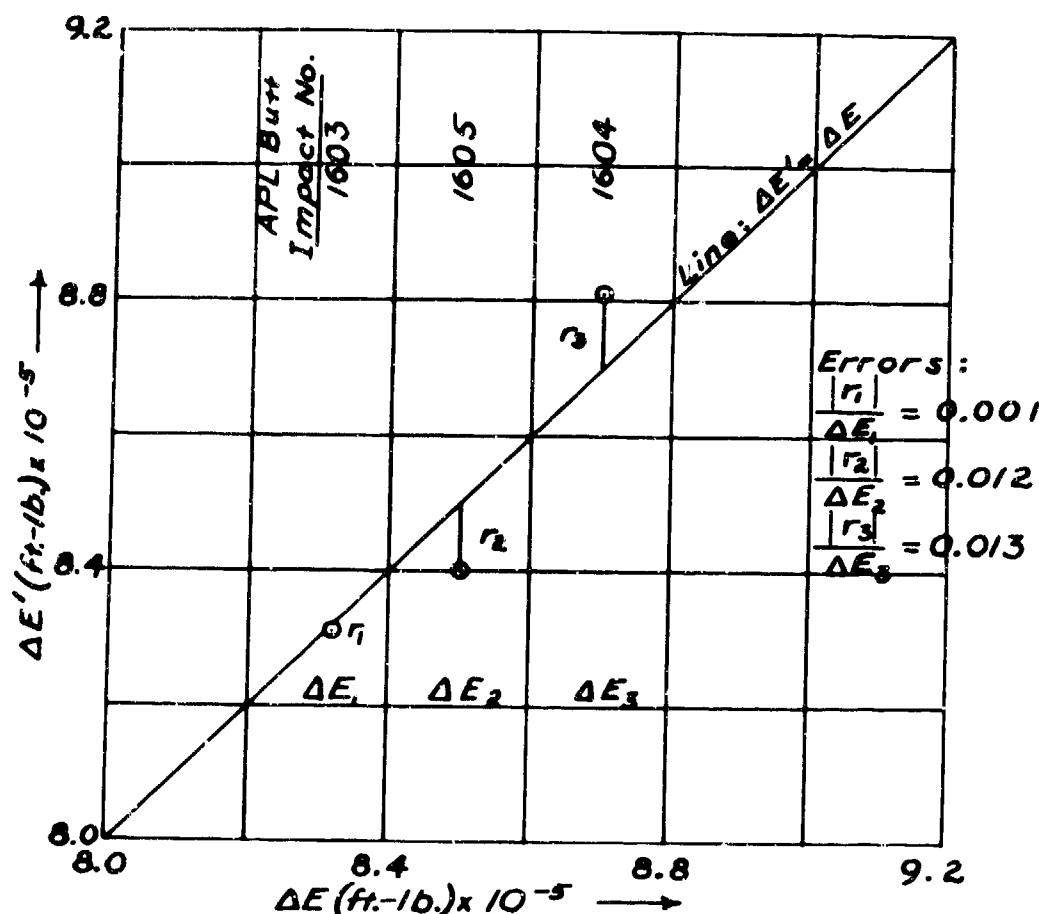
ENERGY ABSORPTION FROM HOLE SIZE
vs.
ENERGY ABSORPTION FROM BALLISTIC DATA

3" AP M79 Projectile vs. 4" Class B plate at 0° obliquity

APL Butt Impact No.	E_s , ft.-lb.	ΔE , ft.-lb.	Hole Diameter Mean d^2	Mean d
1603	8.83×10^5	8.32×10^5	8.912 in. ²	2.985 in.
1604	14.30	8.70	9.478	3.078
1605	11.38	8.50	9.017	3.003

Limit Energy: $E_L = 8.28 \times 10^5$ ft.-lb.

Actual Plate Thickness: $e = 4.07$ in.



$$\Delta E = 0.93 E_L + 0.07 E_s$$

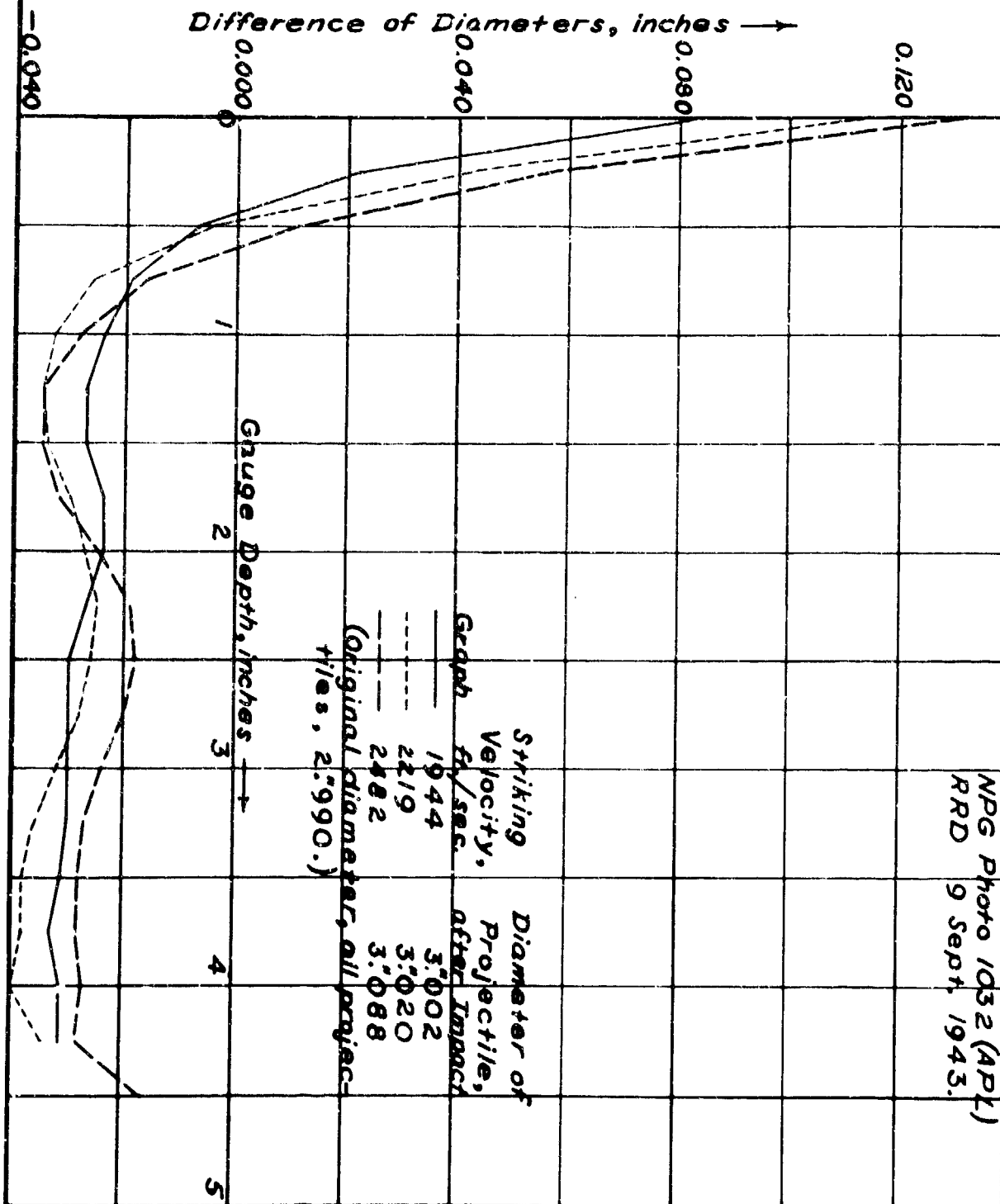
$$\Delta E' = A \bar{d}^2 (e - 0.132 \bar{d})$$

The value of A , determined by least squares to give a best fit in $\Delta E = A \bar{d}^2 (e - 0.132 \bar{d})$, is 2.563×10^4 ft. lb./in.³

Photo 1054 (APL)
10 Sept. 1943

IMPACT HOLE DIAMETER LESS PROJECTILE DIAMETER
3"AP M79 Projectile vs. 4" Class B Plate at 0°

The gauge depth is measured from the plane of the original face of the plate. All penetrations complete.



UNCLASSIFIED

From the measured hole diameters, the corresponding energy value, E_L , has been calculated using equations (1) and (2). The value of A found for this plate is 2.56×10^4 ft. lb./in³. The energy absorbed by the plate is found from the residual energy plot--see Fig. 3 of reference (2), which was obtained by firing at the particular plate in question. The residual - energy graph has the equation

$$E_R = 0.93 (E_S - E_L), \quad \dots \dots \dots (3)$$

from which the energy absorbed is found to be

$$\Delta E = E_S - E_R = 0.93 E_L + 0.07 E_S \quad \dots \dots \dots (4)$$

Fig.2 of this report shows a plot of the energy absorption, for the three rounds gauged in Fig. 1. vs. energy required to make the hole, as calculated from Eq. (1). It will be observed that there is a good correlation. Thus; predictions (1), (2) and (3) given on p. 3 are correct.

Unfortunately the situation is not quite so simple; when the projectiles were recovered and calipered, it was found that they had swelled from their original maximum diameter of 2.99 in., as shown in the following table:

Striking velocity, f.s.	1944	2219	2482
Projectile dia., max., in.	3.002	3.020	3.088

Fig. 3 is a graph of hole-diameter less projectile-diameter against the depth of the hole, measured from the original plane of the face of the plate. It will be observed that when the holes were gauged, they were smaller than the projectile through most of their depth, presumably due to elastic contraction of the plate after passage of the projectile, the difference in diameters being around 0.003.

The reader will doubtless have noticed the curious maxima and minima of diameter, the holes being larger in the middle of the plate than near either the front or back surfaces. No satisfactory explanation has been found for these maxima and minima, nor for the systematic variation in their amplitude and position with the velocity of the projectiles. An obvious first thought was that the fluctuations might be associated with the heating of the plate due to plastic working during impact, and subsequent cooling of different parts of the plate at different rates. The magnitude of the thermal expansions

UNCLASSIFIED

UNCLASSIFIED

UNCLASSIFIED

which can be expected is much too small, however, as the following calculation shows:

The diameter of the worked volume is about 9 in., and the plate thickness is 4 in., so the worked volume is

$$\pi d^2 e / 4 = \pi (9)^2 (4) / 4 = 254 \text{ in.}^3$$

Taking the density of steel as 490 lb./ft.³, the weight of metal plastically worked is thus

$$(254 \text{ in.}^3)(490 \text{ lb./ft.}^3) / (1728 \text{ in.}^3/\text{ft.}^3) = 72 \text{ lb.}$$

The limit velocity of this plate for a 15-lb. projectile is 1885 ft./sec., so the energy absorbed by the plate is about

$$(1/2) m V_L^2 = (1/2)(15/32.2)(1885)^2 = 827,000 \text{ ft.lb.}$$

or

$$1064 \text{ B.T.U.}$$

Taking the specific heat of steel as about 0.115 B.T.U./lb. °F., this could raise the temperature of the plastically-worked metal an average of 128°F. or 71°C. As the coefficient of thermal expansion of steel is about 0.114 x 10⁻⁴ per °C., this would correspond to an expansion of about 0.0024 in. for a 3 inch hole. Actually the situation is more complicated due to non-uniform heating and cooling of the worked material and interference of the unheated part of the plate with the expansion of the worked portion, but it is clear that an expansion of not more than the order of 2.4 mils cannot account for anomalous variations in hole diameter of from 6 to 18 mils.

The fact that both the projectile and the hole which it makes enlarge as the striking velocity increases obscures the details of the mechanism of hole enlargement. The taper of the hole, extending to a depth of more than an inch below the plane of the original surface of the plate, indicates that inertial effects must be able to expand the hole so that the expansion continues even after passage of the projectile. It will be noted in Fig. 3 that the enlargement of the hole in the tapered portion is systematically greater with greater striking velocity. These considerations suggest that dynamic effects directly on the plate are the primary cause of hole enlargement with increased velocity, and that the swelling of the projectile - doubtless produced by the increased forces experienced at higher striking velocities - is an incidental accompaniment. The correctness

UNCLASSIFIED

of this view is supported by indications that the pressure on the after portion of the projectile nose is small - i.e., that the swelled portion of the projectile exerts little force on the plate.

On the other hand, alternative explanations must be admitted as possible. One may argue that the projectile swells on first striking the plate, and that the enlarged projectile then has to make a larger hole to get through the plate. Another possibility is that the deformation of the projectile increases the coefficient of $(1/2) \rho v^2$ in the dynamic term in the pressure, exaggerating the enlargement of the hole by inertial effects.

To decide among these diverse possibilities it is desirable to repeat the experiment on hole enlargement with projectiles of various hardnesses, including some very hard projectiles having an ogival contour resembling that of an ordinary projectile after the latter has been deformed by striking a heavy plate.

III ENERGY EXPENDED IN PROJECTILE DEFORMATION.

The amount of energy in a projectile available for making a hole in a plate is at most the difference between its striking energy and the work done in deforming the projectile. It is clear therefore that, even if the change in projectile conformation did not result in increased resistance by the plate, a deforming projectile would require greater striking energy to penetrate a given plate under given conditions than a non-deforming projectile of the same original dimensions.

It would be highly desirable to know the amount of energy expended in deforming a projectile in any specified way. Except possibly at normal impact, it is doubtful whether the energy of projectile deformation can be calculated by practicable mathematical procedures. However, the deformation energy presumably appears as heat in the projectile, and if the projectile can be recovered quickly enough after impact it should be possible to measure the energy of deformation calorimetrically. Preliminary measurements have been made on several projectiles fired at a 4" Class B plate at various obliquities. As shown below, the projectiles being the 3" AP M-79 solid shot, weighing 15-lb.

UNCLASSIFIED

Fig. 4 - NPG Photo No. 908 (ATL)

(CONFIDENTIAL)



UNCLASSIFIED

UNCLASSIFIED

UNCLASSIFIED

<u>APL Butt</u> <u>Impact No.</u>	<u>Obl.</u> <u>Degrees</u>	<u>Vs</u> <u>ft./sec.</u>	<u>Es</u> <u>ft. lb.</u>	<u>Energy of Deform.</u> <u>B.T.U.</u>	<u>ft. lb.</u>
1516	0°	2000	9.31×10^5	33	26×10^3
1517	0°	1959	8.95×10^5	36	28×10^3
1518	20°	2013	9.45×10^5	69	54×10^3

The results are necessarily approximate. The average elapsed time from impact until immersion of the projectiles in the bucket used as calorimeter was about two minutes. The temperature rise was from about 0.7 to 4° C., depending on the amount of water used and the extent of the projectile deformation. Fig. 4 is a photograph of the projectiles in question; the butt impact numbers are painted on the projectile bodies. Round 1518 shows the greatest deformation observed in this type of projectile without the occurrence of rupture. From the data one can calculate the mean temperature rise in the projectile, which is from about 10° C. to 25° C.; of course, the temperature distribution in the projectile is far from uniform, being greatest in the nose where the projectile experiences the most working.

There are serious practical limitations upon calorimetric work. The projectile must not penetrate into the sand of the butt so deeply that it cannot be recovered quickly, and the sand must be dry. An unknown amount of heat will be generated in the projectile by the scouring it receives in the sand before coming to rest.

IV

FRICITION IN PROJECTILE IMPACT.

It has been assumed in discussions of projectile impact that the friction between the plate-material and the nose of the projectile is small. Zener and Peterson (reference (3)) have discussed friction from a theoretical point of view; they conclude that the high temperature generated at the plate-projectile boundary by plastic working of the plate material will cause the friction to fall to a very low value. This section presents some experimental data from which the order of magnitude of the frictional effects can be estimated.

When a projectile passes through a plate, scratches usually appear upon the body and upon the band, if the latter is still present. It is found that these scratches make a greater angle with the projectile axis than do the engravings made upon the band by the rifling.

UNCLASSIFIED

Thus, if ω_S , V_S represent striking angular and linear velocities of the projectile, respectively, and ω_R , V_R the corresponding residual angular and linear velocities after passage through the plate, the scratches left on body and band after passage through the plate show that

$$\omega_R/V_R > \omega_S/V_S \quad \dots \dots \dots (5)$$

Measurement of the pitch of the scratches made by the plate on the band enables one to estimate ω_R/V_R , from which ω_R can be calculated if V_R is known, which is usually the case in rounds fired at homogeneous plate. As V_S and ω_S are known from the firing record and from the pitch of the rifling, information is available for the calculation of the percentage losses in rotational and translational kinetic energy. Estimation of the pitch of the rifling from the engraving on the band and comparison with the pitch as known from the design of the gun gives a check on the accuracy of the method. The accuracy is not very great, involving errors of around 20% in estimating the pitch of the rifling, which implies errors of 5 - 10% in estimation of ω_R/V_R , where the pitch is much greater. Fortunately no great accuracy is necessary to show the order of magnitude of the frictional effects, as will appear in the course of the subsequent calculations.

As has been pointed out in Part II of this report there is good evidence that the pressure on the projectile nose is not uniform, being greatest at the point and least near the bourrelet. To cover this situation, two calculations will be made - one based on a uniform pressure over the ogive, and the other with the pressure a maximum at the point of the projectile and zero at the bourrelet. A preliminary calculation will be made in which it is assumed that $\omega_R/V_R = \omega_S/V_S$, and this calculation will later be modified to agree with the experimentally established inequality (5).

In the simple case of a solid cylindrical projectile the moment of inertia about the projectile axis is

$$I_0 = mr_0^2/2, \quad \dots \dots \dots (6)$$

where r is the radius of the projectile. For pointed solid shot, I_0 will be somewhat less than indicated in equation (6); for pointed shell it should be about the same. If the projectile makes one turn in 25 calibers - a typical rifling - the angular velocity and linear

UNCLASSIFIED

velocity are related by the equation

$$\omega/2\pi = V/50r_0 \quad \dots \dots \dots (7)$$

so that

$$\omega^2 = (\pi^2/625r_0^2)V^2 \quad \dots \dots \dots (8)$$

The rotational kinetic energy $(1/2) I_0 \omega^2$ is therefore

$$T_\phi = (1/2)(mr_0^2)(\pi^2/625 r_0^2)V^2$$

or

$$T_\phi = (1/2)mV^2(\pi^2/1250) \quad \dots \dots \dots (9)$$

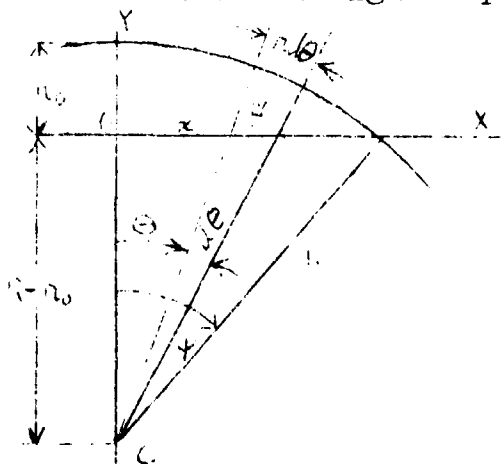
As $\pi^2/1250 = 0.00789$, it is clear that the rotational kinetic energy is somewhat less than 1% of the translational kinetic energy, which latter quantity is symbolized by T_x :

$$T_\phi = 0.00789 T_x \quad \dots \dots \dots (10)$$

If as supposed in this preliminary calculation T_ϕ remains a constant fraction of T_x (i.e., $\omega/V = \text{const.}$), one may also write

$$dT_\phi/dT_x = 0.00789 \quad \dots \dots \dots (11)$$

Suppose a projectile with an ogival nose of radius R , the radius of the projectile at the bourrelet being r_0 . The ogive is generated by revolving an arc of a circle about its chord, and the circle may be described in terms of an angular parameter θ :



$$\left. \begin{aligned} y &= R(\cos\theta - \cos\psi) \\ x &= R \sin \theta \\ \psi &= \arccos (1-r_0/R) \end{aligned} \right\} (12)$$

As the projectile nose is symmetrical about the X-axis, the element of area may be taken as

UNCLASSIFIED

$$dA = 2\pi y ds = 2\pi R(\cos \theta - \cos \psi) R d\theta \dots (13)$$

where the element of arc ds is $R d\theta$.

Suppose the normal pressure on the ogive to be p , and the coefficient of friction to be k . k is probably a function of u , the instantaneous tangential velocity of plate material along the ogival surface, which will vary from point to point, but these variations will be disregarded, so that the value of k calculated will be a sort of average over the surface. For the present it is assumed that p is constant over the surface. The force of friction on an element of area dA will then be

$$kp dA, \dots (14)$$

directed tangential to the surface, and the torque due to the friction on dA will be

$$dM = kpy dA, \dots (15)$$

y being given by equations (12) and dA by equation (13). The total torque on the ogive due to friction is obtained by integrating equation (15) over the ogive:

$$M = \int_0^\psi kpy dA = 2\pi R^3 kp \int_0^\psi (\cos \theta - \cos \psi)^2 d\theta$$

or

$$M = \pi R^3 kp [\psi (1 + 2 \cos^2 \psi) - 3 \sin \psi \cos \psi] \dots (16)$$

In revolving through an angle $d\phi$ the work done by the frictional torque will be $M d\phi$, so that the change in rotational kinetic energy is

$$dT_\phi = - M d\phi \dots (17)$$

with M given by equation (16).

The force of friction on an element of area dA being $kp dA$, and tangential to the surface, the component of this frictional force parallel to the projectile axis is $kp dA \cos \theta$. the total resistance due to friction on the ogive is thus

$$F = \int_0^\psi kp \cdot 2\pi R^2 (\cos \theta - \cos \psi) d\theta \cdot \cos \theta$$

$$= 2\pi R^2 kp \int_0^\psi (\cos^2 \theta - \cos \theta \cos \psi) d\theta$$

or

UNCLASSIFIED

$$F = \pi R^2 k p (\psi - \sin \psi \cos \psi), \dots (18)$$

and is of course opposite to the direction of motion. For a uniform pressure the resisting force due to the normal pressure, resolved along the projectile axis, is

$$P = \pi r_o^2 p, \dots (19)$$

also opposite to the direction of motion. The total loss in energy of translation due to the resisting forces when the projectile moves a distance dx is

$$dT_x = - (P + F) dx, \dots (20)$$

or

$$dT_x = - [\pi r_o^2 p + \pi R^2 k p (\psi - \sin \psi \cos \psi)] dx.$$

Factoring, one obtains

$$dT_x = - \pi r_o^2 p [1 + k(R/r_o)^2 (\psi - \sin \psi \cos \psi)] dx. \dots (21)$$

The ratio of dT_ϕ to dT_x is given by equation (11), on the assumption that ω/V is constant, and $d\phi/dx = \pi/25r_o$ for 1:25 rifling. Thus equation (17) is to be divided by equation (21):

$$\frac{dT_\phi}{dT_x} = \frac{R^3 k p [\psi (1 + 2 \cos^2 \psi) - 3 \sin \psi \cos \psi] d\phi}{r_o^2 p [1 + k(R/r_o)^2 (\psi - \sin \psi \cos \psi)] dx}$$

substitution for $d\phi/dx$ and performance of indicated cancellations yields

$$\frac{dT_\phi}{dT_x} = \frac{\pi R^3 k [\psi (1 + 2 \cos^2 \psi) - 3 \sin \psi \cos \psi]}{25 r_o^3 [1 + k(R/r_o)^2 (\psi - \sin \psi \cos \psi)]} \dots (22)$$

Numerical results may now be introduced. For a projectile of the 3" M-79 nose shape, $R/r_o = 10/3$. The value of dT_ϕ/dT_x may be taken as 0.01. $\psi = \arccos(1 - r_o/R)$, $\psi = \arccos(0.7) = 45.5$ or 0.794 radians. A sufficient approximation may be obtained by taking $\psi = \pi/4$, so that $\sin \psi = \cos \psi = 0.707$.

UNCLASSIFIED

UNCLASSIFIED

Substitution in equation (22) yields

$$0.01 = \frac{\pi \cdot 1000 \cdot k(\pi/2 - 3/2)}{25 \cdot 27 [1 + k(100/9)(\pi/4 - 1/2)]} \quad \dots (22a)$$

or

$$0.01 = 0.33 k / (1 + 3.17k)$$

$$\text{whence } k = 0.033 \quad \dots (23)$$

From equations (20) and (21) it can be seen that the ratio of the frictional force to the pressure force is $k(R/r_0)^2 (\psi - \sin\psi \cos\psi)$, or $3.17 k$. Using the value of k from equation (23) it appears that

$$F/P = 3.17k = 0.105 \quad \dots (24)$$

i.e., the frictional force is approximately 10% of the total force acting on the projectile.

This calculation was made using three special assumptions, namely:

- (1) The moment of inertia of the projectile is that of a solid cylinder of the same mass and radius.
- (2) The pitch of the rifling is 1:25 -- a fairly steep pitch for modern high velocity guns.
- (3) During penetration the angular and linear velocities decrease at the same rate, proportional to their initial values.

As pointed out before, assumption (1) will lead to too high values of I_0 for solid shot. Assumption (2) must be adjusted in any actual case to account for the actual pitch of the rifling. Assumption (3) is definitely wrong for actual cases, as it is known that $\omega_R/V_R > \omega_S/V_S$. It is clear therefore that equation (24) places a reasonable upper limit on the effect of friction for the case of uniform pressure, and that from a practical point of view the frictional effect is negligible. However, the measurements of one actual case will be introduced to show the effect of corrections to assumptions (1) to (3); the case is that of a 3" AP M-79 solid shot fired through a 4" Class B plate at 0° Obliquity, as follows:

UNCLASSIFIED

Gun: 3"/50 Cal., rifling 1 turn in 32 calibers
 Striking Velocity, 1959 ft./sec.
 Residual Velocity, 509 ft./sec.

Band and body scratches showed that after emerging from the back of the plate the projectile was turning at a rate of 2.50 radians per foot of advance, or one turn in 10 calibers. Thus, during penetration $d\phi/dx$ varies between $\pi/32$ and $\pi/10$; leaving the value at $\pi/25$ will correct somewhat for the change in "pitch" in passing through the plate, yet favor a large value of k -- i.e., the value of k will be an upper limit.

The mean value of dT_ϕ/dT_x may be calculated from the available data as follows:

Let $T_{\phi,S}$ and $T_{\phi,R}$ be respectively the striking and residual kinetic energies of rotation and $T_{x,S}$ and $T_{x,R}$ the corresponding kinetic energies of translation. Then

$$T_{\phi,S} - T_{\phi,R} = (I_0/2)(\omega_S^2 - \omega_R^2) \dots (25)$$

and

$$T_{x,S} - T_{x,R} = (m/2)(V_S^2 - V_R^2) \dots (26)$$

Using $I_0 = mr_0^2/2$, $\omega_S = (\pi/32r_0)V_S$, and

$\omega_R = (\pi/10r_0)V_R$, one finds that

$$\frac{T_{\phi,S} - T_{\phi,R}}{T_{x,S} - T_{x,R}} = \frac{\pi^2}{2} \frac{[(V_S/32)^2 - (V_R/10)^2]}{V_S^2 - V_R^2} \dots (27)$$

and this is the mean value of dT_ϕ/dT_x during penetration. Using $V_S = 1959$, $V_R = 509$ in equation (27) it is thus found that

$$dT_\phi/dT_x = 0.00160 \dots (28)$$

When this value is used in the left member of equation (22c), it is found that

$$k = 0.0049 \dots (29)$$

and

$$F/P = 0.0156. \dots (30)$$

All calculations made so far have been based upon the assumption of a constant pressure over the ogive, whereas there is good reason to suppose that the pressure is greatest at the point of the projectile and decreases towards the bourrelet, the exact mode of variation being however unknown. The general effect of a non-uniform pressure can be exhibited conveniently by choosing a mode of variation which will give a maximum pressure on the projectile axis (i.e., the point) and a zero pressure at the greatest diameter (i.e., the bourrelet). A suitable pressure distribution is

$$p = p_0 (\sin \theta / \sin \psi), \quad \dots \dots \dots (31)$$

a distribution which has the additional advantage of simplifying the necessary integrals. The pressure force resolved parallel to the projectile axis is

$$\begin{aligned} P &= \int_0^\psi P dA \sin \theta \\ &= \int_0^\psi P_0 (\sin \theta / \sin \psi) \cdot 2\pi R^2 (\cos \theta - \cos \psi) d\theta \cdot \sin \theta \\ &= (2\pi R^2 P_0 / \sin \psi) (\sin^3 \theta / 3 - (\cos \psi) (\theta - \sin \theta \cos \theta / 2)) \Big|_0^\psi \end{aligned}$$

or

$$P = (2\pi R^2 P_0 / \sin \psi) \left[(\sin^3 \psi) / 3 - \cos \psi (\psi - \sin \psi \cos \psi) / 2 \right] \quad (32)$$

The friction force, calculated as in equation (18), is

$$\begin{aligned} F &= \int_0^\psi p k dA \cos \theta \\ &= (2\pi R^2 P_0 k / \sin \psi) \int_0^\psi \sin \theta (\cos \theta - \cos \psi) \cos \theta d\theta \\ &= (2\pi R^2 P_0 k / \sin \psi) \left[\cos \psi (\cos^2 \theta / 2 - \cos^3 \theta / 3) \right]_0^\psi, \\ \text{or } F &= (2\pi R^2 P_0 k / \sin \psi) \left[\cos^3 \psi / 6 - \cos \psi / 2 + 1/3 \right] \dots \dots \dots (33) \end{aligned}$$

The torque due to friction is

$$\begin{aligned} M &= \int_0^\psi p k dA y \\ &= \int_0^\psi (P_0 k \sin \theta / \sin \psi) 2\pi R^2 (\cos \theta - \cos \psi) d\theta R (\cos \theta - \cos \psi) \\ &= (2\pi R^3 k P_0 / \sin \psi) \int_0^\psi (\cos \theta - \cos \psi)^2 \sin \theta d\theta \end{aligned}$$

whence

UNCLASSIFIED

$$M = (2\pi R^3 k p_0 / 3 \sin \psi) (1 - \cos \psi)^3 \dots (34)$$

From this point the calculation proceeds as in the previous uniform-pressure case, using the basic equation

$$\frac{dT_\phi}{dT_x} = \frac{M d\phi}{(P + F) dx} \dots (35)$$

By comparison of equations (32), (33), and (34) it is seen that the factor $(2\pi R^2 p_0 / \sin \psi)$ cancels from numerator and denominator of equation (35). Substitution from equations (32), (33), and (34) in (35) therefore yields

$$\frac{dT_\phi}{dT_x} = \frac{\pi}{25 r_0} \cdot \frac{R}{3} \cdot \frac{k(1 - \cos \psi)^3}{A(\psi) + k B(\psi)} \dots (36)$$

where

$$A(\psi) = (\sin \psi)^3 / 3 - \cos \psi (\psi - \sin \psi \cos \psi) / 2$$

and

$$B(\psi) = 1/3 - \cos \psi (1 - \cos^2 \psi / 3) / 2$$

As before, let $\psi = \pi/4$ radians, $\sin \psi = \cos \psi = 0.707$, and $R/r_0 = 10/3$. In the actual case previously used as an example, dt_ϕ/dT_x may be taken as 0.00160, giving

$$0.00160 = \frac{\pi}{75} \cdot \frac{10}{3} \cdot \frac{0.0251 k}{0.0169 + 0.0387 k}, \dots (37)$$

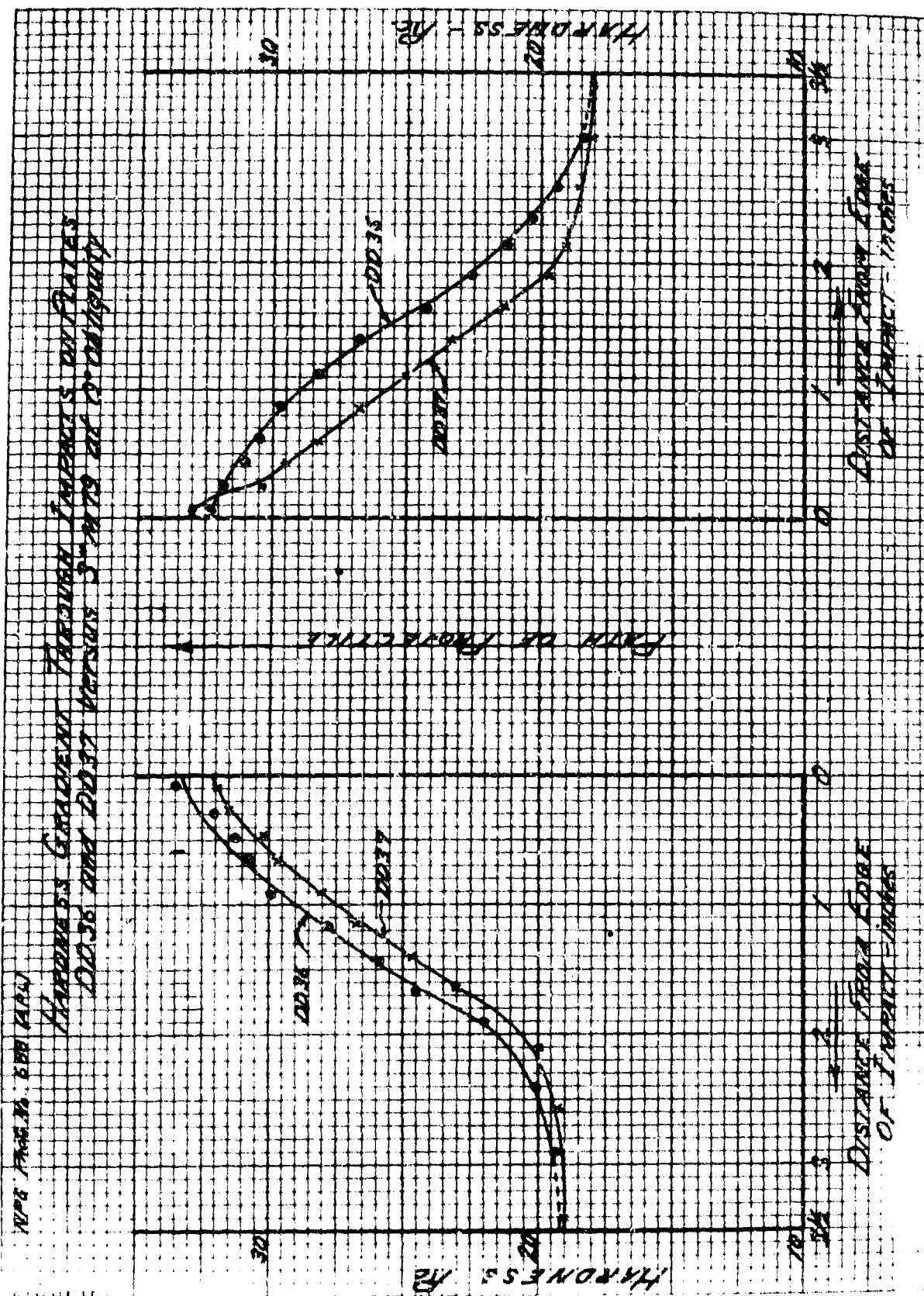
whence

$$k = 0.00785, \dots (38)$$

and

$$F/P = 3.87 k / 1.69 = 0.018. \dots (39)$$

Thus, the frictional force is rather less than 2% of the total force acting.

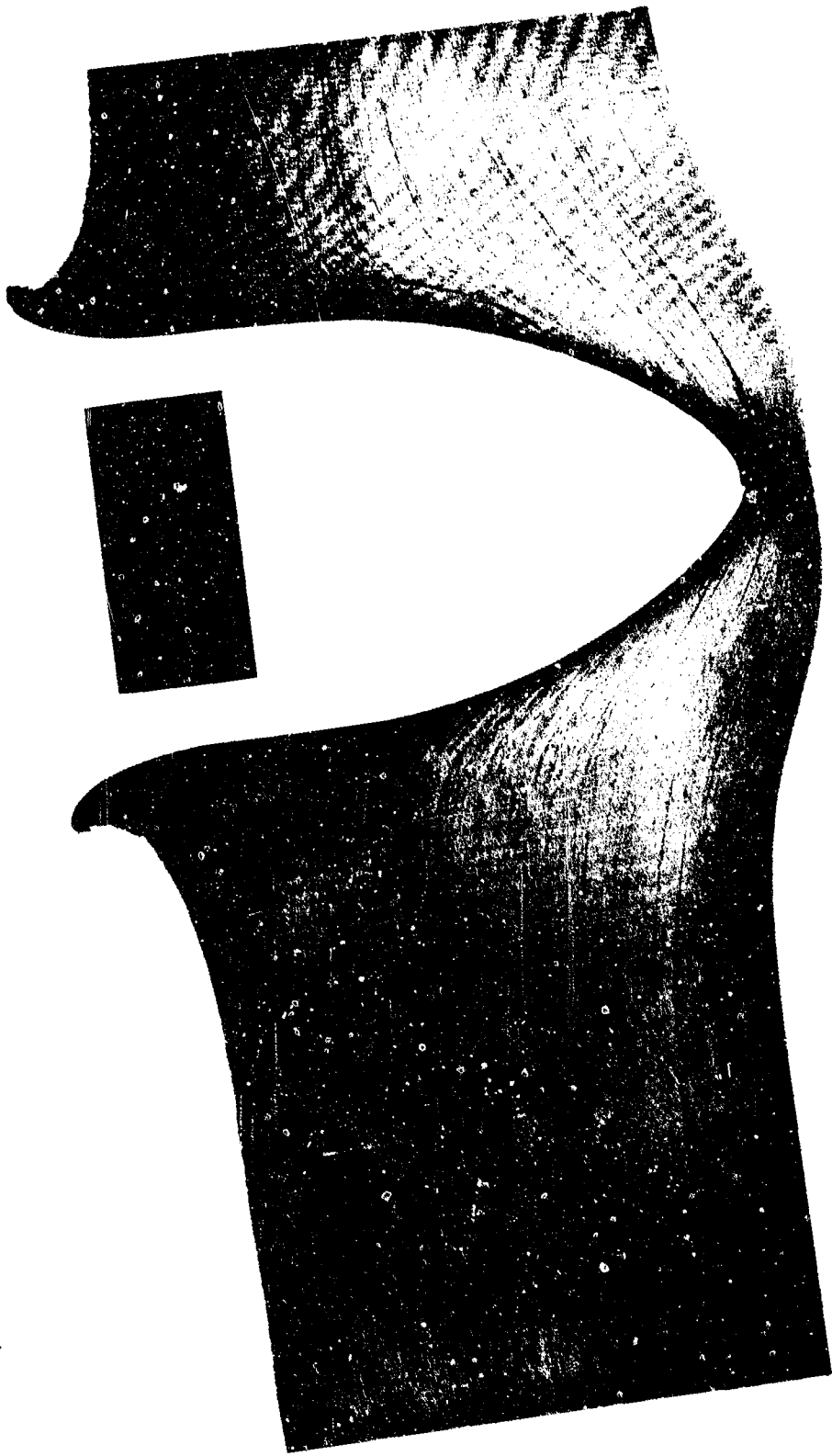


NPG PHOTO NO. 890 (APL).
Impact in 4" Class B Armor Plate. Macroetched section
of Impact #698, APL Plate #115. Projectile: 3" AP
4"; Etch: 38 HCl, 12 H₂SO₄, 50 H₂O; 160° F. - 3-4 hours.
7 July 1943

UNCLASSIFIED



MPG PHOTO NO. 892 (APL) - Impact in 4" Class B Armor Plate. Macro-
etched section through axis of impact #697, APL Plate #115. Pro-
jectile: 3" AP M79; Penetration: 5"; Etch: 38 HCl, 12 H₂SO₄.
50 H₂O; 160° F.; 3-4 hours.
7 July, 1943.



NPS PHOTO NO. 891 (APL) - Impact in 4" Class B Armor Plate. Macro-
etched section through axis of Impact #700, APL Plate #115. Pro-
jectile: 3" AP M79; Penetration: 2-1/2"; Etch: 38 HCl., 12 H₂SO₄,
50 H₂O; 160° F. 3-4 hours.
7 July, 1943.

UNCLASSIFIED



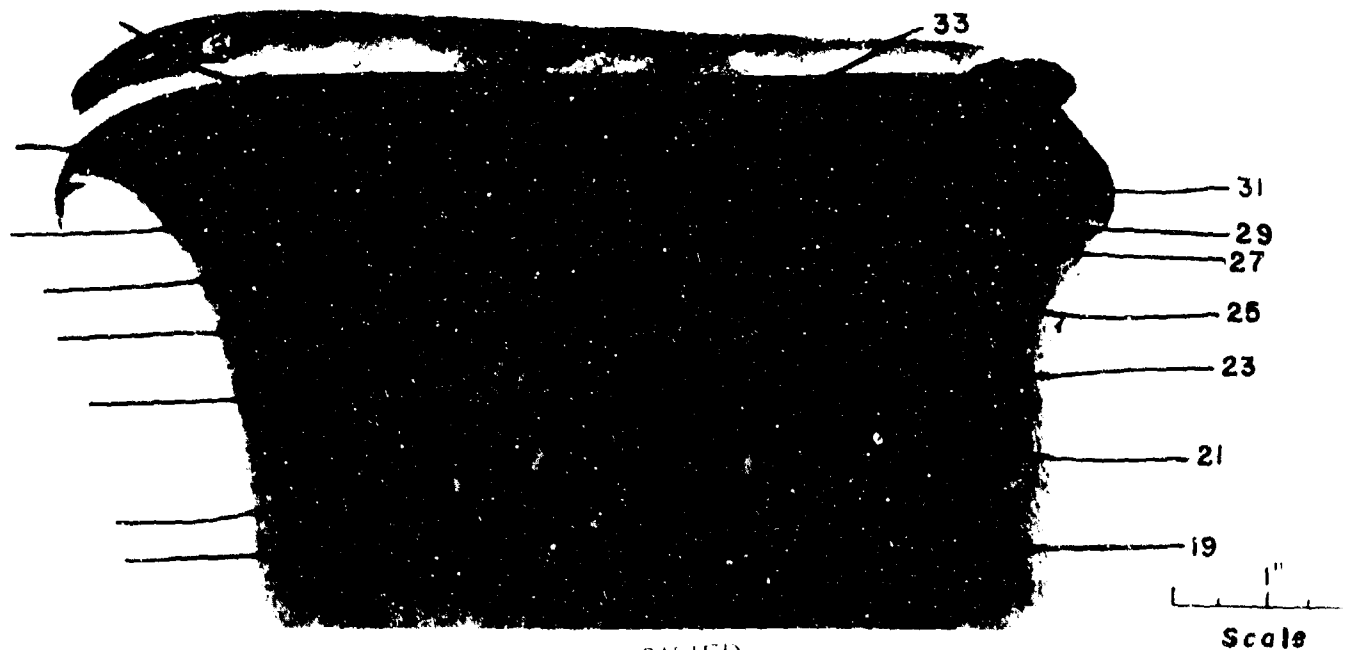
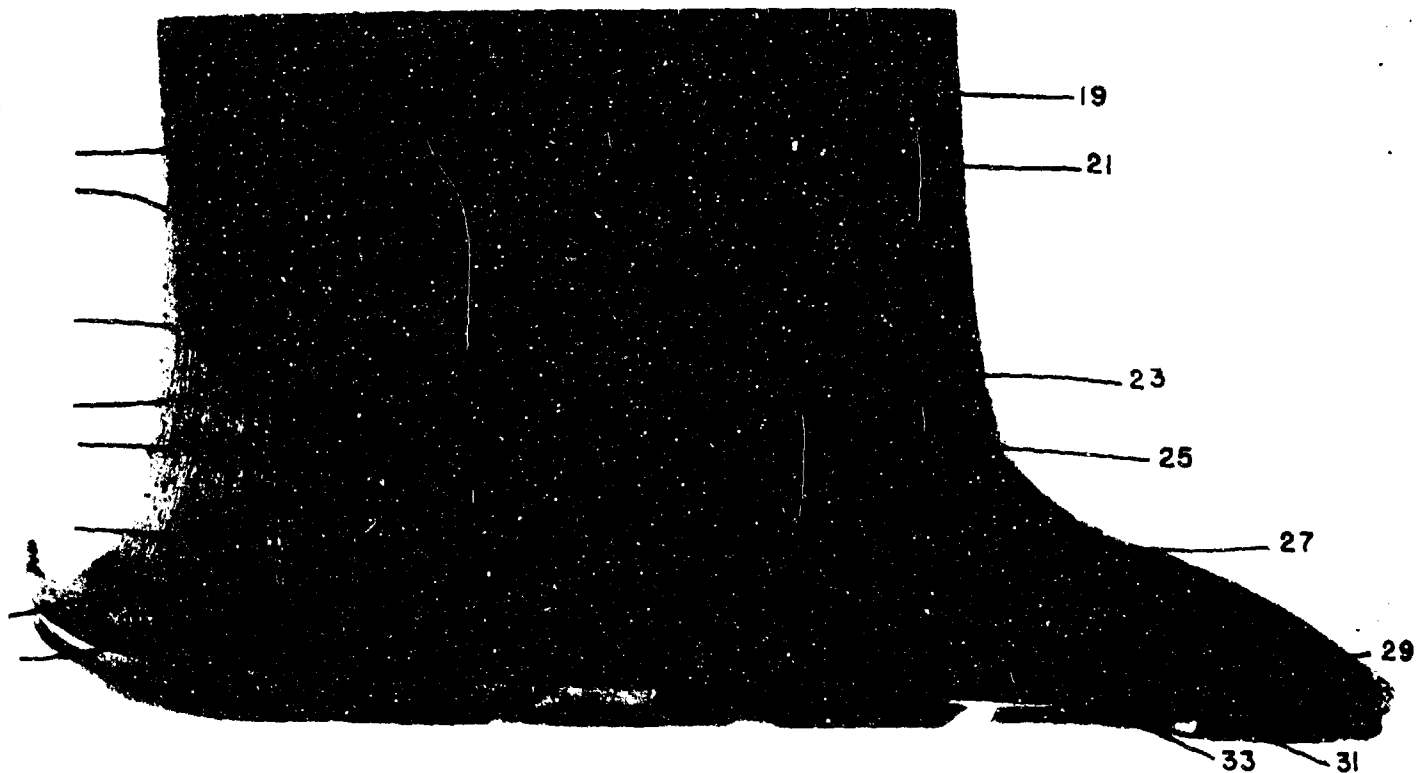
NPG PHOTO NO. 893 (APL).
Impacts in 4" Class B Armor Plate. Macroetched section through axis
of Impact #702, APL Plate #115. Projectile: 3" AP M79; Penetration:
1-1/2"; Etch: 38 HCl, 12 H₂SO₄, 50 H₂O; 160° F; 3-4 hours.
7 July 1943.

DECLASSIFIED



NPG Photo No. 919 (APL) UNCLASSIFIED

ISOSCLERIC LINES ON A CROSS SECTION OF APL IMPACT NO. 1080
C.I. Plate No. DD36 vs. 3" M79-0° Obliquity
Rockwell C Hardness Indicated



UNCLASSIFIED

Scale

ISOSCLERIC LINES ON A CROSS SECTION OF APL IMPACT NO. 765
C.I. Plate No. DD 37 vs. 3" M79--0° Obliquity
Rockwell C Hardness Indicated



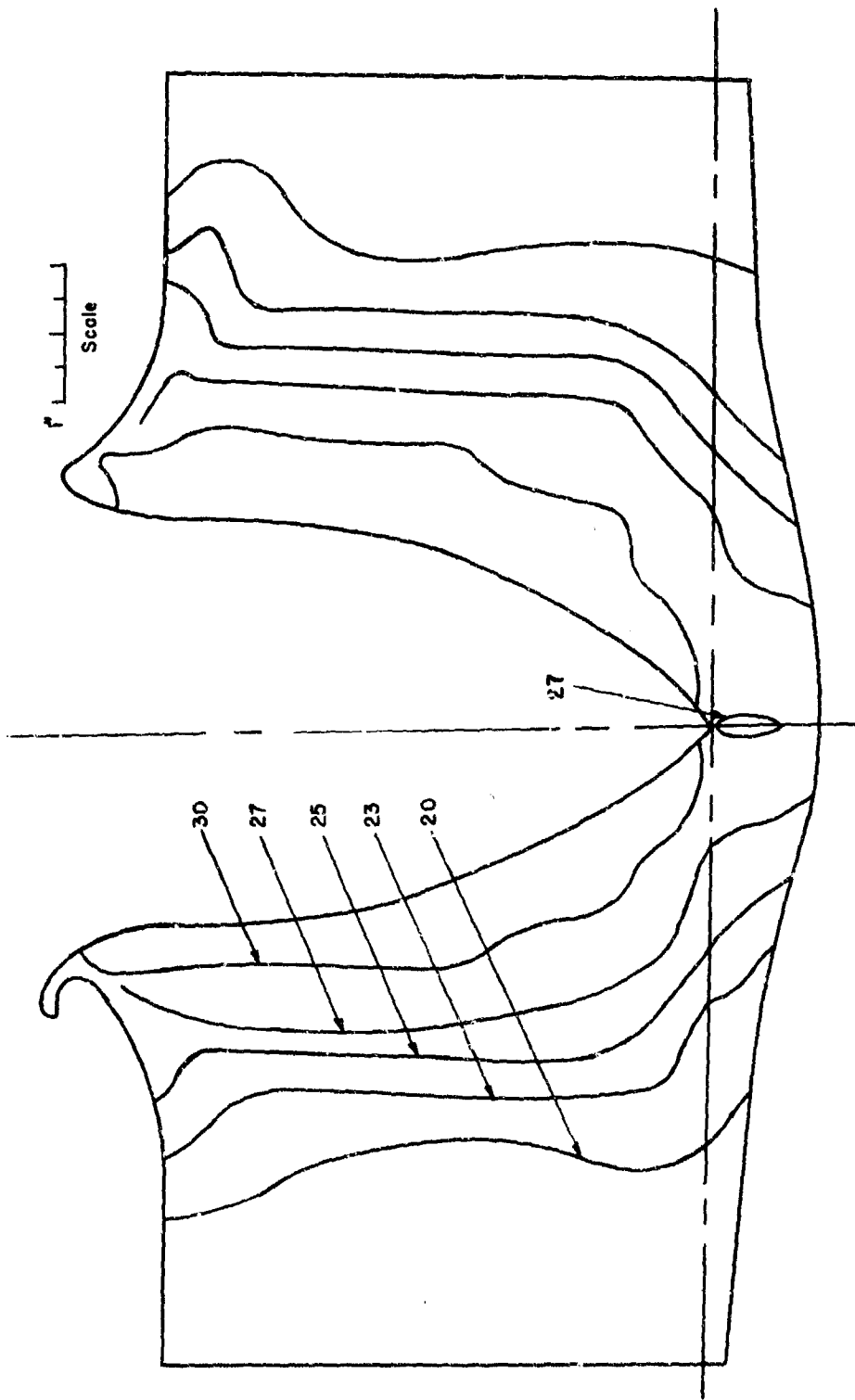
Path of Projectile →




1"
Scale

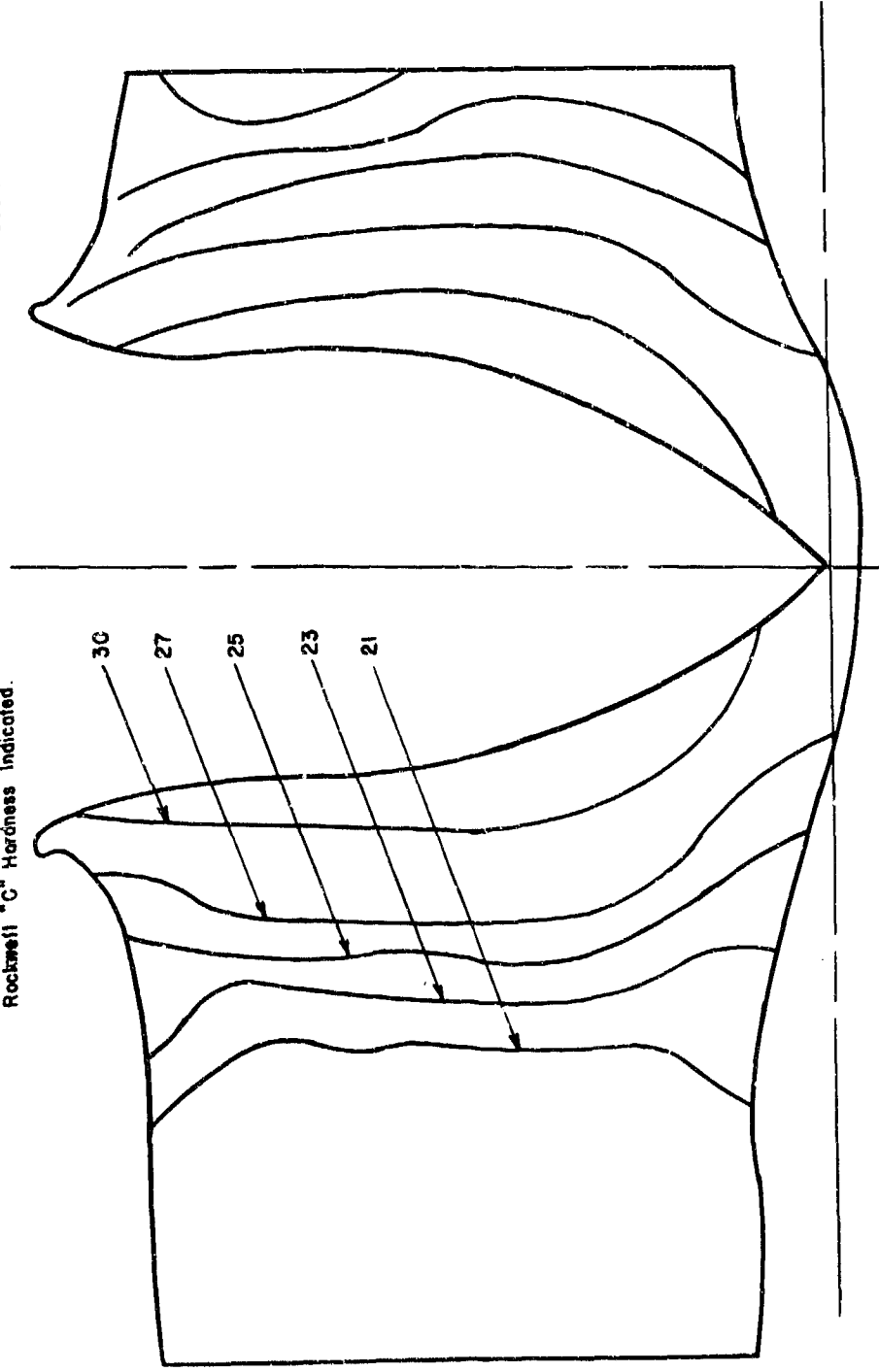
UNCLASSIFIED

NP.G. Photo No. 863 (APL)
ISOSCLERIC LINES ON A CROSS SECTION OF APL IMPACT No. 698
4" Class "B" Armor vs. 3" AP M79 0° Obliquity
APL Plate No. 115 Penetration 4"
Rockwell "C" Hardness Indicated

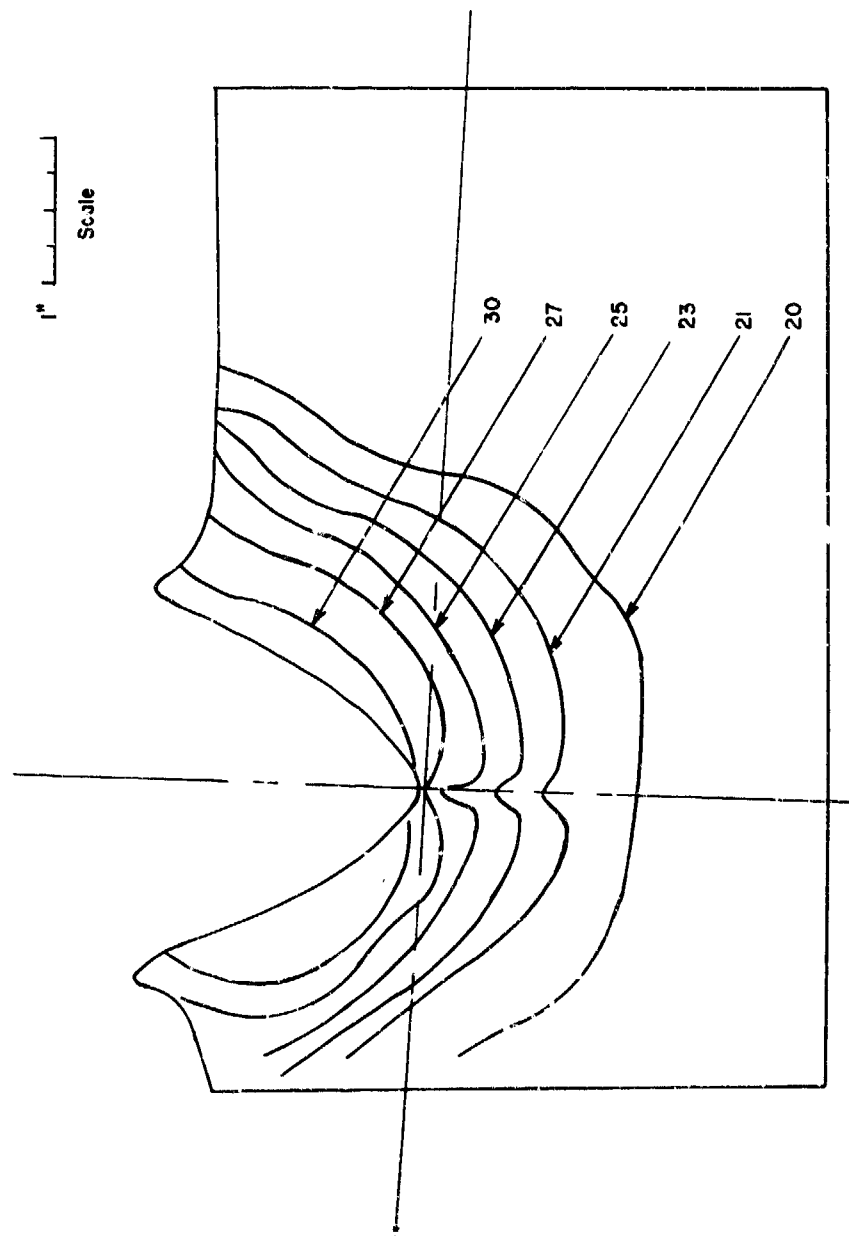


NPG Photo No. 864 (APL)
 ISOSCLERIC LINES ON A CROSS SECTION OF APL IMPACT NO. 697
 4" Class "B" Armor vs. 3" AP M79 - 0° Obliquity
 APL Plate No. 115 Penetration 5
 Rockwell "C" Hardness Indicated.

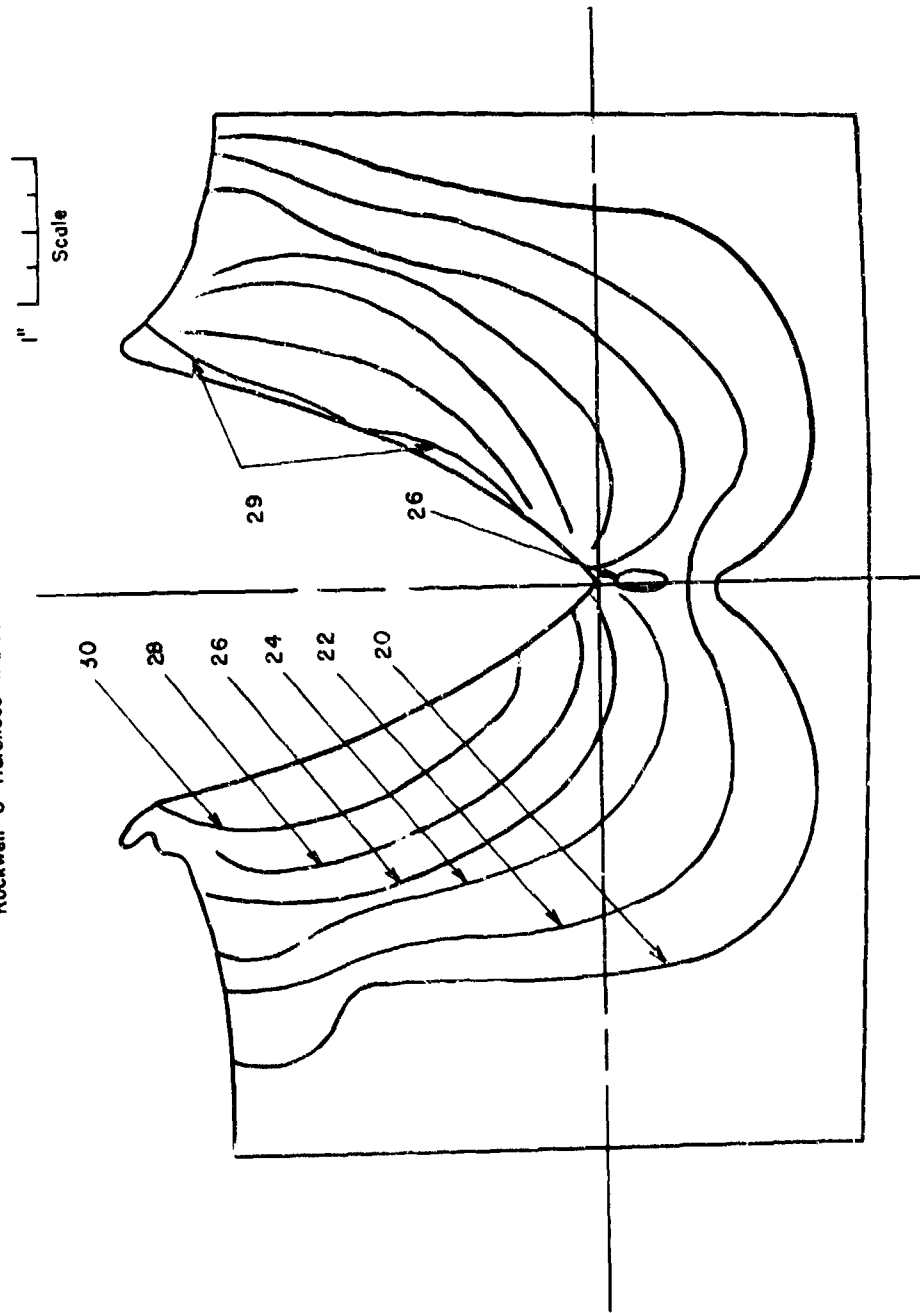
1"  Scale

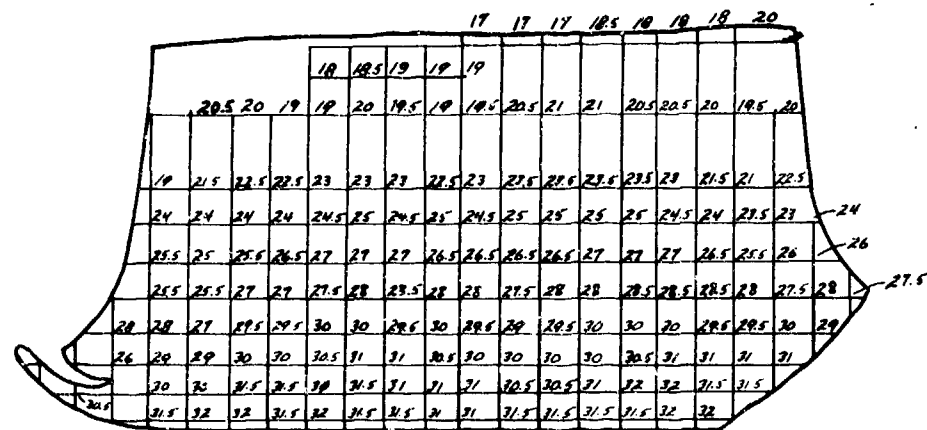


N.P.G. Photo No. 861 (APL)
 ISOSCLERIC LINES ON A CROSS SECTION OF APL IMPACT NO. 102
 of Class "B" Armor vs. 3" AP M79 - 0° Obliquity
 APL Plate No. 115 Penetration 1 1/2
 Rockwell "C" Hardness Indicated

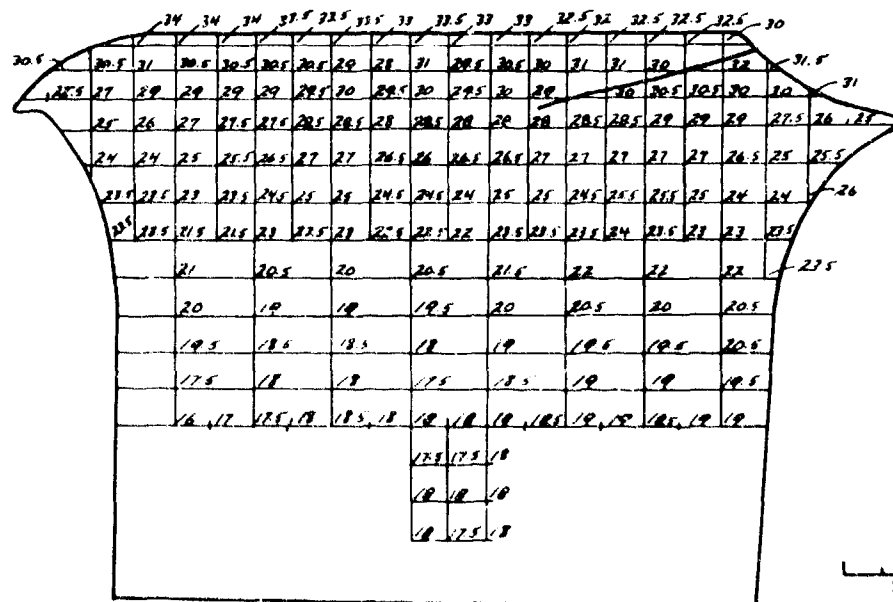


N.P.3. Photo No. 862 (APL)
 ISOSCLERIC LINES ON A CROSS SECTION OF APL IMPACT No. 700
 4" Class "B" Armor vs. 3" AP M79 0° Obliquity
 APL Pl. 3 No. 115 Penetration 2 1/2"
 Rockwell "C" Hardness Indicated





Path of Projectile

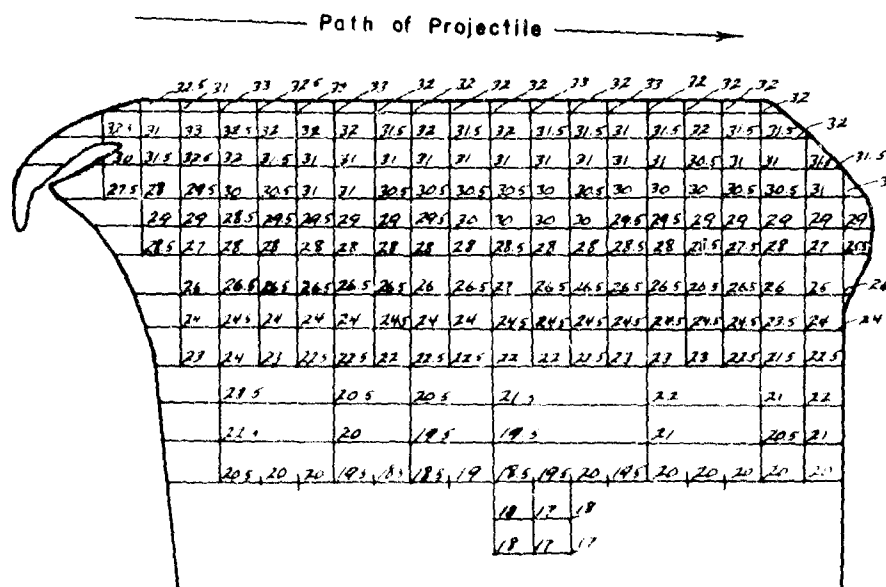
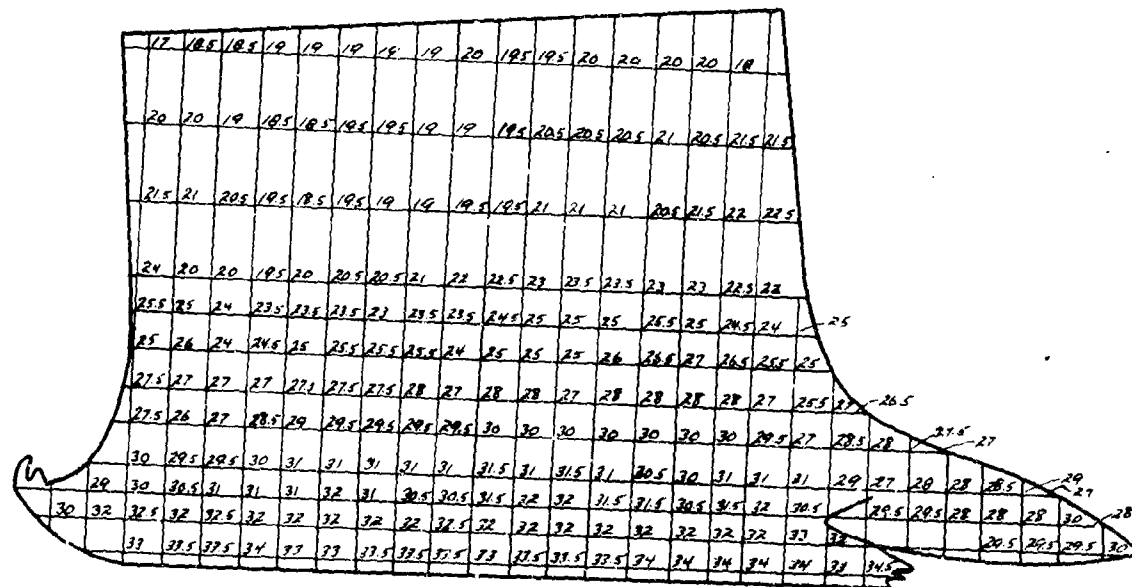


Scale

UNCLASSIFIED

NPG Photo No. 687 (APL)

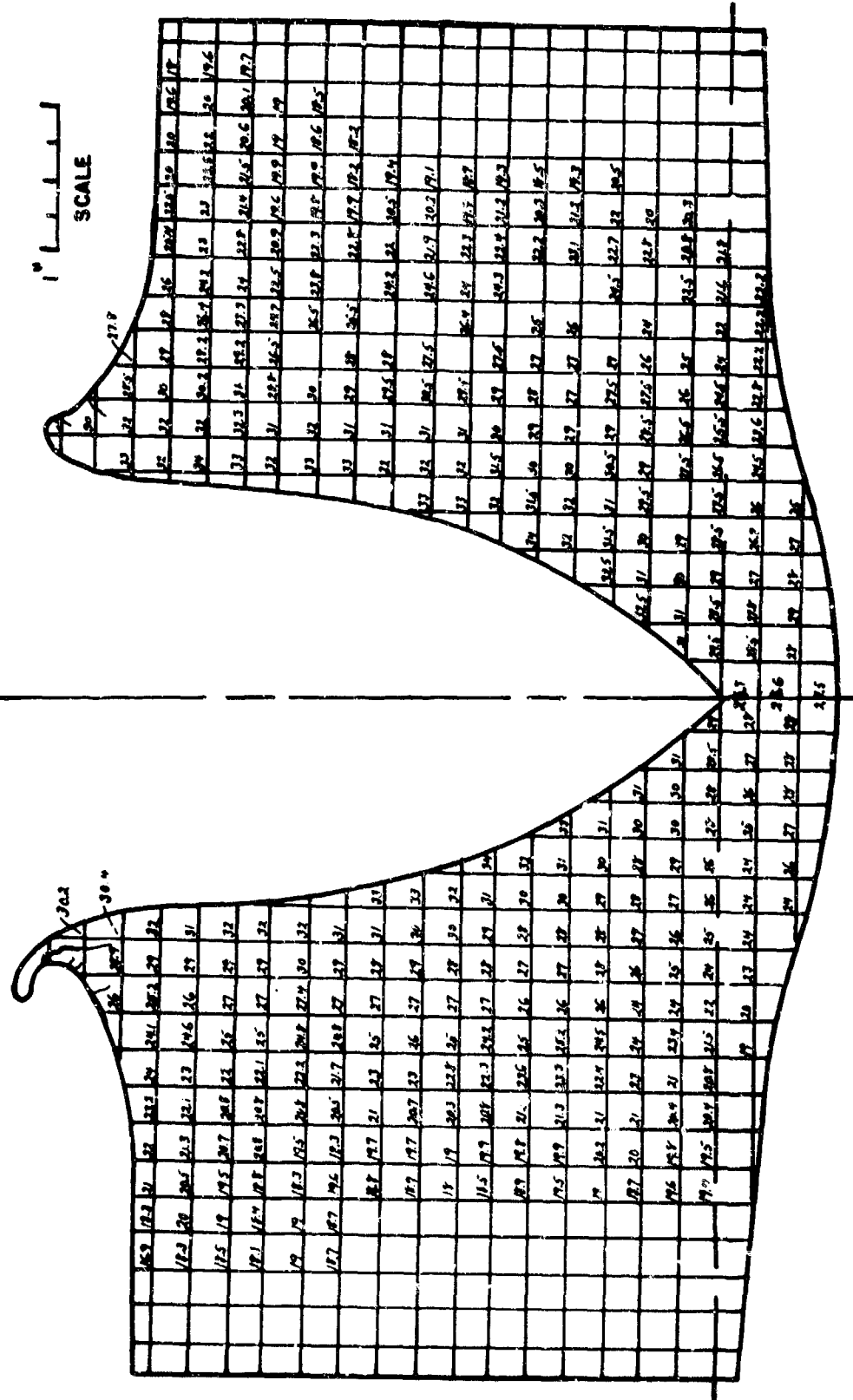
ROCKWELL C HARDNESS DISTRIBUTION
ON A CROSS SECTION THROUGH APL IMPACT NO. 1080
Carnegie Illinois Plate No. DD36 Versus
3" M 79 at 0° Obliquity



1"
Scale

N.P.G. Photo No. 1006

ROCKWELL "C" HARDNESS DISTRIBUTION
ON A CROSS SECTION OF IMPACT No. 698
4" Class "B" Armor vs. 3" AP M79-0° Obliquity
APL Plate No.115

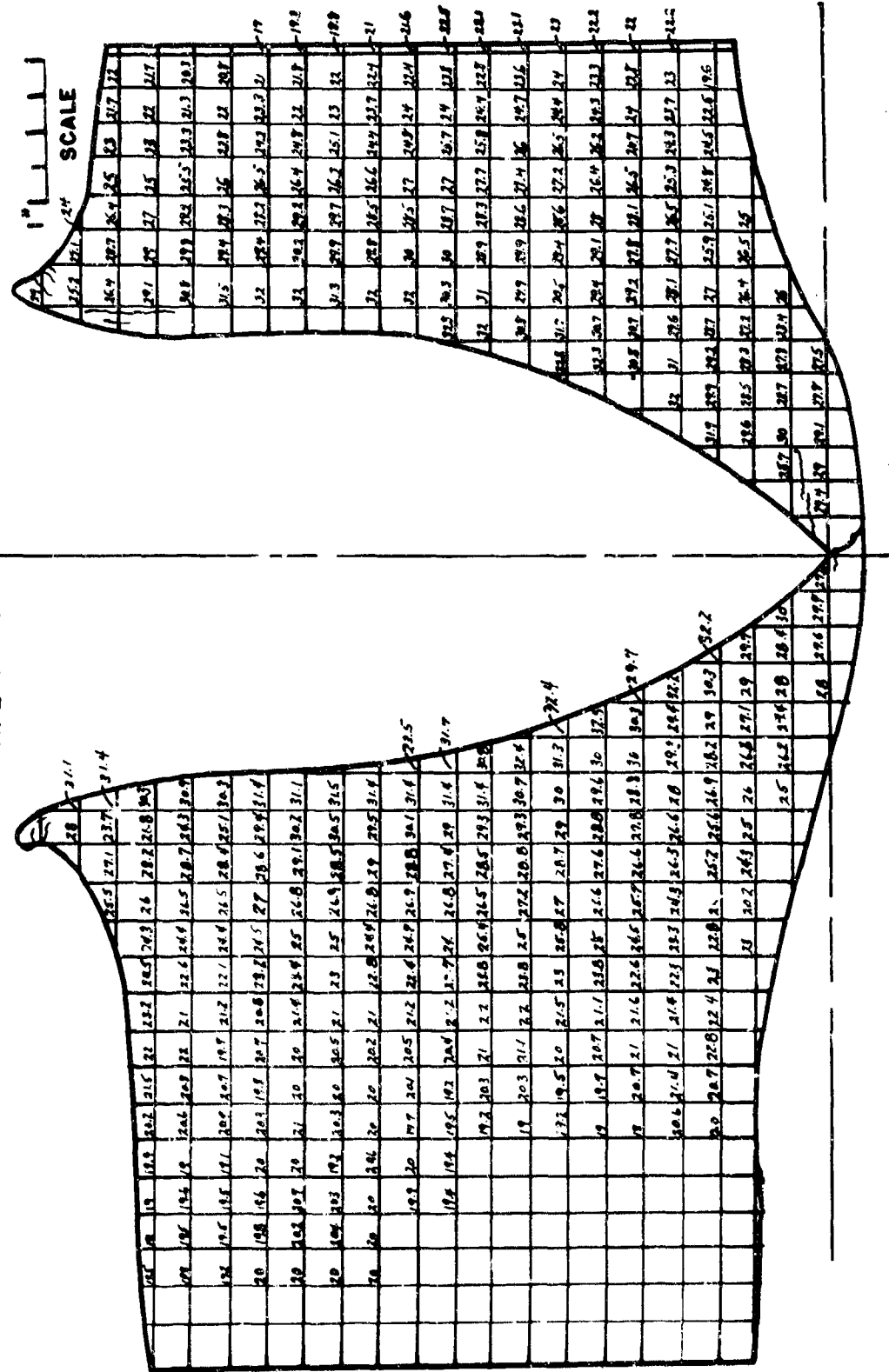


UNCLASSIFIED

N.P.G. Photo No. 1007

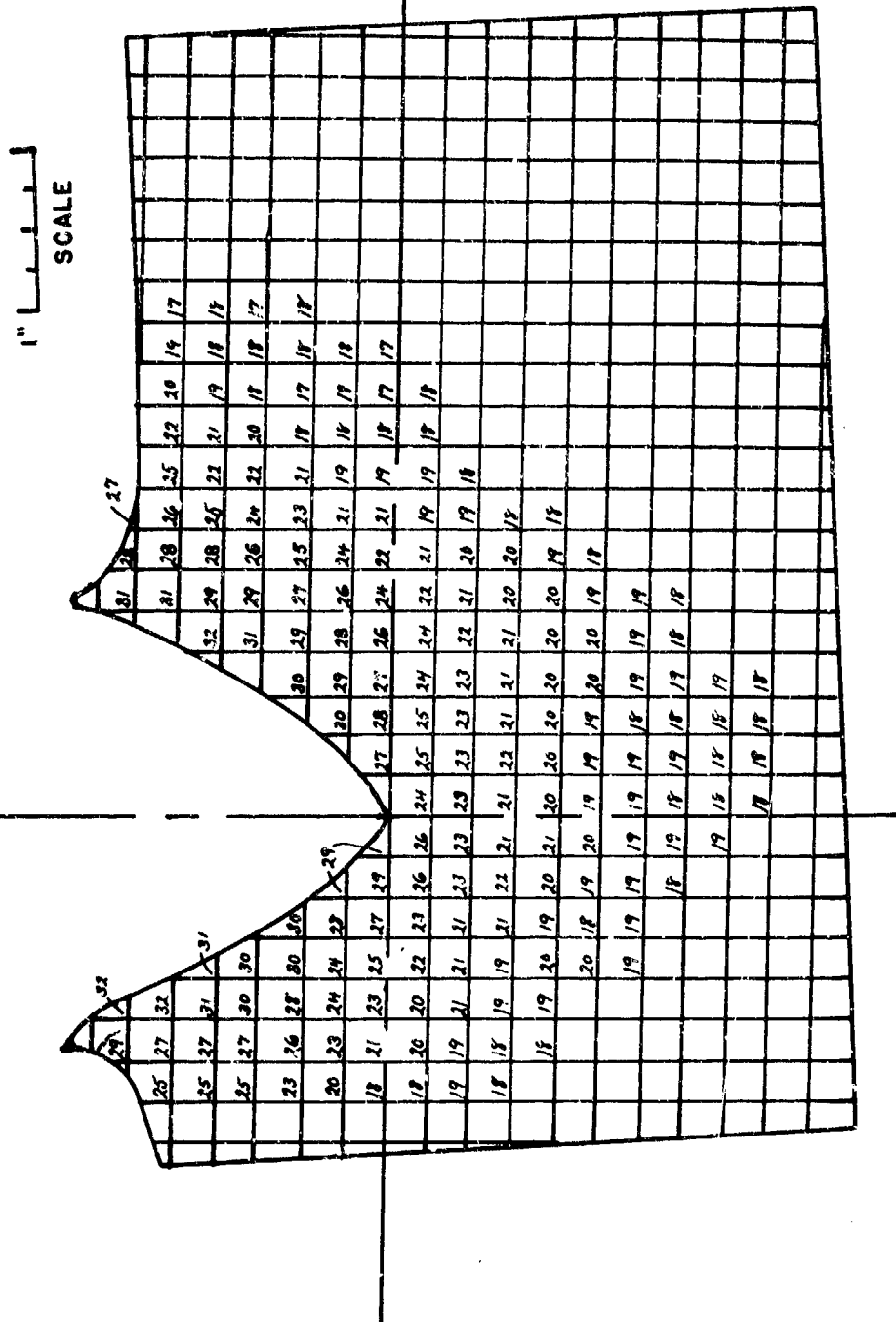
ROCKWELL "C" HARDNESS DISTRIBUTION
ON A CROSS SECTION OF IMPACT No. 697
4" Class "B" Armor vs. 3" AP M79 - 0° Obliquity

APL Plate No. 115



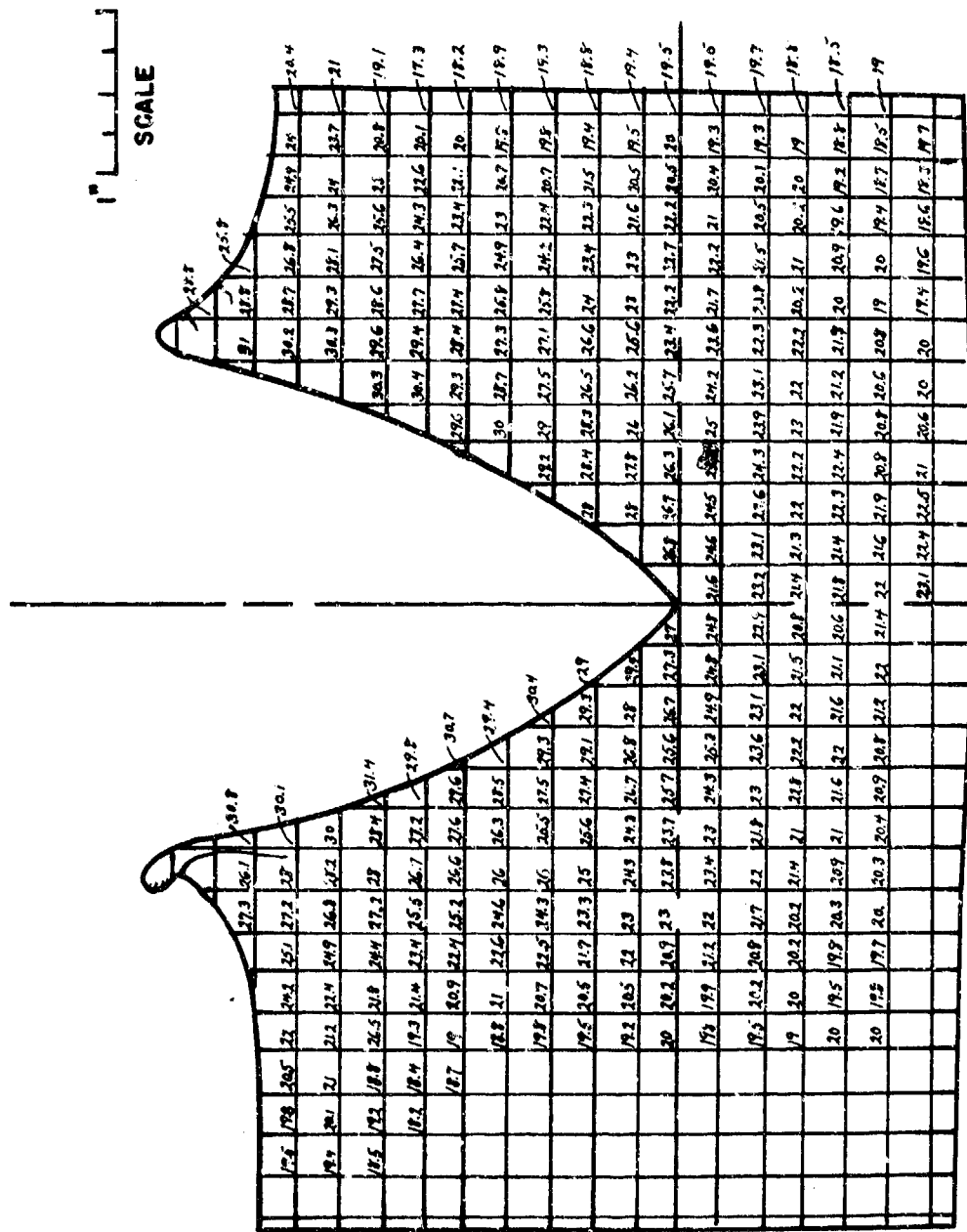
N.P.G. Photo No. 1004

ROCKWELL "C" HARDNESS DISTRIBUTION
ON A CROSS SECTION OF APL IMPACT No. 702
4" Class "B" Armor vs. 3" AP M79 - 0° Obliquity
APL Plate No. 115



N.P.G. Photo No. 1005

ROCKWELL "C" HARDNESS DISTRIBUTION
ON A CROSS SECTION OF IMPACT NO. 700
4" Class "B" Armor vs. 3" AP M79 - 0° Obliquity
APL Plate No. 115



On the assumption of uniform pressure over the ogive it was found that $F/P = .0156$ (equation (30)); assuming the pressure a maximum at the point of the projectile and zero at the bourrelet, it appears that $F/P = 0.018$. It is clear that the more the pressure is concentrated towards the point of the projectile, the greater will be the calculated effect of friction for a particular observed dT_ϕ/dT_x . The particular case chosen as an example may be regarded as typical of the usual values of dT_ϕ/dT_x . It seems safe to assume, therefore, that friction contributes rather less than 2% to the total resisting force on the projectile, the figure of 2% being regarded as an upper bound, the probable value being lower. In the present state of our knowledge of penetration mechanisms sufficient accuracy is obtained in calculation if the effect of friction is disregarded.

V. HARDNESS DISTRIBUTION AROUND IMPACTS.

In reference (2) it was remarked that hardness surveys and etchings of sections of impacts give considerable support to the applicability of Bethe's thin-plate theory to plates up to an e/d value of 1.36, insofar as the effect of petalling is ignored. Figures 5 to 10 show hardness patterns for a series of incomplete and complete penetrations in 4" Class B plates. Figures 11 to 16 show the lines of equal hardness (isoscleric lines) across these sections, which presumably determine isoscleric surfaces in the plate symmetrical about the projectile axis. Figures 15 to 20 show etchings of the sections. Figure 21 is a graph showing the hardness gradient across a typical section through a complete penetration.

A study of these figures reveals certain important facts, namely:

- (1) Plate material is squeezed out laterally and out of the face of the plate, as envisaged by Bethe's theory. A "neutral plane" is apparent somewhat nearer the face of the plate than the back.
- (2) In the etched views, it is apparent that while Bethe's mechanisms is applicable to the body of the plate, there is a narrow zone adjacent to the hole where the plate material is dragged forward by the projectile. The width of this zone increases through the plate, merging into the petalling zone at the back.

UNCLASSIFIED

- (3) In the incomplete penetrations, the isoscleric surfaces parallel the surface of the hole, justifying the view that adjacent to the projectile, the principle displacement is normal to the surface of the projectile nose.
- (4) The diameter of the work-hardened region is approximately three calibers.
- (5) In the complete penetrations, the general parallelism of the isoscleric lines to the projectile axis is in accord with Bethe's theory.
- (6) In the incomplete penetrations, note the small amount of work hardening directly ahead of the projectile nose.

UNCLASSIFIED

UNCLASSIFIED

REFERENCES

1. Frankford Arsenal Report of 23 May, 1941:
"Attempt of a Theory of Armor Penetration",
by H. A. Bethe.
2. Naval Proving Ground Report 1-43: Penetra-
tion Mechanisms I. The penetration of Homo-
geneous Armor by Uncapped Projectiles at 0°
Obliquity.
3. Watertown Arsenal Report 710/492. Mechanism
of Armor Penetration - Second Partial Report,
by C. Zener and R. A. Peterson.

UNCLASSIFIED